Free Piston Expansion Tube," *Proceedings 18th International Symposium on Shock Tubes and Waves* (Sendai, Japan, July 1991), Springer-Verlag, 1992.

[4]Tamagno, J., Bakos, R., Pulsonetti, M., and Erdos, J., "Hypervelocity Real Gas Capabilities of GASL's Expansion Tube (HYPULSE) Facility," AIAA Paper 90-1390, June 1990.

[5]Wilson, G. J., "Time-Dependent Quasi-One Dimensional Simulations of High Enthalpy Pulse Facilities," AIAA Paper 92-5096, Dec. 1992.

[6]Meyer, R. F., "The Impact of a Shock Wave on a Movable Wall," *Journal of Fluid Mechanics,* Vol. 3, No. 3, 1957, pp. 309–323.

[7]Courant R., and Friedrichs, K. O., *Supersonic Flow and Shock Waves,* Applied Mathematical Sciences, Vol. 21, Springer-Verlag, New York, 1976, pp. 97–106.

[8]Jacobs, P. A., "Quasi-One-Dimensional Modeling of Free-Piston Shock Tunnels," AIAA Paper 93-0352, Jan. 1993.

[9]Tamagno, J., private communication, General Applied Science Laboratories, Ronkonkoma, NY, July 1992.

[10]Bittker, D. A., and Scullin, V. J., "General Chemical Kinetics Computer Program for Static and Flow Reactions, with Application to Combustion and Shock Tube Kinetics," NASA TN-D-6586, Jan. 1972.

[11]Sagnier, P., and Marraffa, L., "Parametric Study of Thermal and Chemical Nonequilibrium Nozzle Flow," *AIAA Journal,* Vol. 29, No. 3, 1991, pp. 334–343.

[12]Hall, J. G., Eshenroeder, A. Q., and Marrone, P. V., "Blunt-Nose Inviscid Airflows with Coupled Nonequilibrium Processes," *Journal of the Aerospace Sciences,* Vol. 29, No. 9, 1962, pp. 1038–1051.

[13]Lordi, J. A., and Mates, R. E., "Nonequilibrium Effects on High-Enthalpy Expansions of Air," *AIAA Journal,* Vol. 3, No. 10, 1965, pp. 1972–1974.

[14]Harris, C., "Comment on 'Nonequilibrium Effects on High-Enthalpy Expansions of Air'," *AIAA Journal,* Vol. 4, No. 6, 1966, p. 1148.

Sensitivity Derivatives for Three-Dimensional Supersonic Euler Code Using Incremental Iterative Strategy

Vamshi Mohan Korivi,* Arthur C. Taylor III,† and Gene W. Hou‡
Old Dominion University, Norfolk, Virginia 23529
and
Perry A. Newman§ and Henry E. Jones¶
NASA Langley Research Center, Hampton, Virginia 23681

Introduction

In recent work,[1,2] an incremental strategy was proposed to iteratively solve the very large systems of linear equations that are required to obtain quasianalytical sensitivity derivatives from advanced computational fluid dynamics (CFD) codes. The technique was successfully demonstrated for two large two-dimensional problems: a subsonic and a transonic airfoil. The principal feature of this incremental iterative strategy is that it allows the use of the identical approximate coefficient matrix operator and algorithm to solve the nonlinear flow and the linear sensitivity equations; at convergence, the accuracy of the sensitivity derivatives is not compromised. This feature allows a comparatively straightforward extension of the methodology to three-dimensional problems; this extension is successfully demonstrated in the present study for a space-marching solution of the three-dimensional Euler equations over a Mach 2.4 blended wing-body configuration.

Received June 29, 1993; presented in open forum at the AIAA 11th Computational Fluid Dynamics Conference, Orlando, FL, July 6–9, 1993; revision received Nov. 5, 1993; accepted for publication Nov. 6, 1993.

*Graduate Research Assistant, Department of Mechanical Engineering.
†Assistant Professor, Department of Mechanical Engineering. Member AIAA.
‡Associate Professor, Department of Mechanical Engineering. Member AIAA.
§Senior Research Scientist, Computational Science Branch, Fluid Mechanics Division, MS 159.
¶Research Scientist, U.S. Army Aeroflightdynamics Directorate, JRPO, MS 159. Senior Member AIAA.

Theoretical Background

Discretization of the Euler equations and the boundary conditions results in a large system of coupled nonlinear algebraic equations; for a steady-state solution, this system is represented as

$$\boldsymbol{R}[\boldsymbol{Q}(\boldsymbol{D}), \boldsymbol{D}] = 0 \tag{1}$$

where $\boldsymbol{Q}$ is the vector of field variables and $\boldsymbol{D}$ is a vector of input (design) variables. Differentation of Eq. (1) yields the matrix equation

$$\frac{\mathrm{d}\boldsymbol{R}}{\mathrm{d}\boldsymbol{D}} = \frac{\partial \boldsymbol{R}}{\partial \boldsymbol{Q}}\boldsymbol{Q}' + \frac{\partial \boldsymbol{R}}{\partial \boldsymbol{D}} = 0 \tag{2}$$

where $\boldsymbol{Q}' \equiv \mathrm{d}\boldsymbol{Q}/\mathrm{d}\boldsymbol{D}$. The linear Eq. (2) must be solved for $\boldsymbol{Q}'$ for the subsequent computation of the sensitivity derivatives of the aerodynamic output functions $\boldsymbol{F}$ with respect to the input variables $\boldsymbol{D}$:

$$\boldsymbol{F} = \boldsymbol{F}[\boldsymbol{Q}(\boldsymbol{D}), \boldsymbol{D}] \tag{3}$$

Differentiation of Eq. (3) yields

$$\frac{\mathrm{d}\boldsymbol{F}}{\mathrm{d}\boldsymbol{D}} = \frac{\partial \boldsymbol{F}}{\partial \boldsymbol{Q}}\boldsymbol{Q}' + \frac{\partial \boldsymbol{F}}{\partial \boldsymbol{D}} \tag{4}$$

where $\mathrm{d}\boldsymbol{F}/\mathrm{d}\boldsymbol{D}$ are the sensitivity derivatives of interest.

The standard incremental formulation for iteratively solving the nonlinear Eq. (1) is

$$-\frac{\tilde{\partial}\boldsymbol{R}^n}{\partial \boldsymbol{Q}}\Delta\boldsymbol{Q} = \boldsymbol{R}^n$$

$$n = 1, 2, 3, \ldots \tag{1}$$

$$\boldsymbol{Q}^{n+1} = \boldsymbol{Q}^n + \Delta\boldsymbol{Q}$$

With typical CFD methods, the coefficient matrix operator $\tilde{\partial}\boldsymbol{R}^n/\partial\boldsymbol{Q}$ represents only a very rough approximation of the exact Jacobian matrix that would be associated with a strict implementation of Newton-Raphson (NR) iteration. Because of memory limitations, NR iteration is not currently feasible on modern supercomputers (with the use of in-core solvers) for Euler and/or Navier-Stokes codes when applied to large two-dimensional and practical three-dimensional flow problems. This computational difficulty carries over to the linear sensitivity equations, Eq. (2); as a remedy, these equations should be cast into an incremental form and solved iteratively as

$$-\frac{\tilde{\partial}\boldsymbol{R}}{\partial \boldsymbol{Q}}\Delta\boldsymbol{Q}' = \frac{\mathrm{d}\boldsymbol{R}^m}{\mathrm{d}\boldsymbol{D}} = \frac{\partial \boldsymbol{R}}{\partial \boldsymbol{Q}}\boldsymbol{Q}'^m + \frac{\partial \boldsymbol{R}}{\partial \boldsymbol{D}}$$

$$m = 1, 2, 3, \ldots \tag{6}$$

$$\boldsymbol{Q}'^{m+1} = \boldsymbol{Q}'^m + \Delta\boldsymbol{Q}'$$

Comparison of Eqs. (6) with Eqs. (5) reveals that the identical left-hand side, approximate coefficient matrix operator and algorithm can be used to iteratively solve the nonlinear flow equation [Eqs. (1)] and the linear sensitivity equation [Eqs. (2)]. Thus, only a change of the right-hand side is required to solve the sensitivity equations. A more complete discussion of the computational advantages of this procedure is given in Refs. 1 and 2.

Sample Problem

The three-dimensional Euler equations are solved here for a fully supersonic flow with the space-marching method described

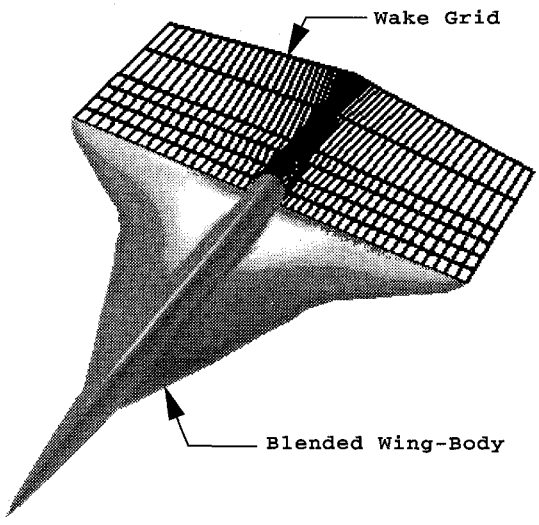

Fig. 1 HSCT 24E blended wing-body configuration.

Table 1 Computational timing comparisons

Solutions	Number of solutions	Ratio
Baseline	1	1.000[a]
Forward finite difference	3	3.426
Quasianalytical	3	0.487

[a]Baseline solution run time for (R^n_{rms}/R^1_{rms}) reduction to $\varepsilon = 10^{-8}$ on Cray-2 is 827 s.

Table 2 Force (C) and moment (C_M) coefficients

C_x (≈ drag)	0.0044
C_y (≈ side)	$\mathcal{O}(\varepsilon)$
C_z (≈ lift)	−0.0133
C_{M_x} (roll)	$< \mathcal{O}(\varepsilon)$
C_{M_y} (pitch)	0.0055
C_{M_z} (yaw)	$< \mathcal{O}(\varepsilon)$

in Ref. 3. The method is an upwind, cell-centered, finite volume scheme that is higher order accurate (second order streamwise and third order in cross plane) and fully conservative in all directions including the streamwise (marching) direction. The method is locally "time iterative" in each cross plane with a spatially split, approximate factorization approach. The Mach 2.4 blended wing-body surface definition was processed with the method given in Ref. 4 and the volume grid subsequently generated by the same authors. Figure 1 is a view of the high speed civil transport (HSCT) 24E blended wing-body configuration, including the wake portion of the computational grid (37 streamwise × 121 circumferential × 15 normal). Grid refinement studies to determine the adequacy of the computed solutions for modeling detailed physical aspects of the flow have not been carried out. This study addresses the consistency of solution sensitivity derivatives computed by two different means, and this consistency is independent of the grid. However, well-converged solutions are required to verify this consistency.

As a consequence of the incremental iterative formulation, the linear sensitivity equations are solved for the sensitivity derivatives of the field variables in each cross plane with the identical space-marching algorithm that is used to solve the nonlinear flow equations. Table 1 shows computational timing comparisons for calculation of sensitivity derivatives using both forward finite differences and the incremental iterative quasianalytical method; all of the timings are given in terms of a baseline time. The measure of convergence levels used for all solutions is given in the footnote to Table 1. Force and moment coefficients for the flight condition Mach (number) = 2.4, α (angle of attack) = 0 deg, and β (yaw angle) = 0 deg are shown in Table 2. Sensitivity derivatives of six output functions (C_x, C_y, C_z, C_{M_x}, C_{M_y}, C_{M_z}) with respect to Mach number, angle of attack, and yaw angle, are given in Table 3. Calculated sensitivity derivative ratios, forward finite differences (perturbation size, $\Delta D = 1.E{-}05$) to quasianalytical derivatives, are shown in Table 4; these ratios are seen to be unity, to four significant figures. However, the computational cost of the finite difference method is approximately seven times greater.

Table 3 Sensitivity derivatives (SD) of force and moment coefficients (quasianalytical incremental iterative strategy)

SD	Design variables, D		
	Mach no.	α	β
$\frac{dC_x}{dD}$	−0.0024	−0.0225	$\mathcal{O}(\varepsilon)$
$\frac{dC_y}{dD}$	$<\mathcal{O}(\varepsilon)$	$\mathcal{O}(\varepsilon)$	−0.0614
$\frac{dC_z}{dD}$	+0.0079	+1.4714	$\mathcal{O}(10\varepsilon)$
$\frac{dC_{M_x}}{dD}$	$< \mathcal{O}(\varepsilon)$	$< \mathcal{O}(\varepsilon)$	−0.0094
$\frac{dC_{M_y}}{dD}$	−0.0033	−0.3244	$\mathcal{O}(10\varepsilon)$
$\frac{dC_{M_z}}{dD}$	$< \mathcal{O}(\varepsilon)$	$\mathcal{O}(\varepsilon)$	−0.0009

Table 4 Sensitivity derivative (SD) ratios, finite difference/quasianalytical, except terms of $\mathcal{O}(\varepsilon)$

$\frac{SD_{FD}}{SD_{QA}}$	Design variables, D		
	Mach no.	α	β
$\frac{dC_x}{dD}$	0.9999	1.0000	a
$\frac{dC_y}{dD}$	a	a	0.9999
$\frac{dC_z}{dD}$	0.9999	1.0000	a
$\frac{dC_{M_x}}{dD}$	a	a	0.9999
$\frac{dC_{M_y}}{dD}$	0.9999	1.0000	a
$\frac{dC_{M_z}}{dD}$	a	a	0.9999

[a]Ratio for extremely small quantities is meaningless.

Conclusions

A computationally efficient general methodology has been successfully demonstrated for iteratively solving the very large systems of linear equations required for obtaining quasianalytical sensitivity derivatives from three-dimensional CFD codes.

Acknowledgment

This research was partially supported by Grant NAG-1-1265 from NASA Langley Research Center.

References

[1]Korivi, V. M., Taylor, A. C., III, Newman, P. A., Hou, G. J.-W., and Jones, H. E., "An Approximately-Factored Incremental Strategy for Calculating Consistent Discrete Aerodynamic Sensitivity Derivatives," *Proceedings of the Fourth AIAA/USAF/NASA/OAI Symposium on Multidisciplinary Analysis and Optimization* (Cleveland OH), AIAA, Washington, DC, 1992, pp. 465–478 (AIAA Paper 92-4746).

[2]Newman, P. A., Hou, G. J.-W., Jones, H. E., Taylor, A. C., III, and Korivi, V. M., "Observations on Computational Methodologies for Use in Large-Scale Gradient-Based Multidisciplinary Design," *Proceedings of the Fourth AIAA/USAF/NASA/OAI Symposium on Multidisciplinary Analysis and Optimization* (Cleveland OH), AIAA, Washington, DC, 1992, pp. 531–542 (AIAA Paper 92-4753).

[3]Newsome, R. W., Walters, R. W., and Thomas, J. L., "An Efficient Strategy for Upwind Relaxation Solutions to the Thin-Layer Navier-Stokes Equations," *AIAA Journal*, Vol. 27, No. 9, 1989, pp. 1165, 1166; also AIAA Paper 87-1113, June 1987.

[4]Barger, R. L., and Adams, M. S., "Automatic Computation of Wing-Fuselage Intersection Lines and Fillet Inserts with Fixed-Area Constraint," NASA TM 4406, March 1993.

Swirl Control in an S-Duct at High Angle of Attack

P. F. Weng*
Shanghai Jiao Tong University, Shanghai 200030, People's Republic of China
and
R. W. Guo†
Nanjing University of Aeronautics and Astronautics, Nanjing 210016, People's Republic of China

Introduction

A DIFFICULT design problem occurs with military aircraft where the inlet is located in an offset position. The problem of angular swirl flow in an S-shaped inlet without guide vanes has come to the fore in the past several years.[1,2] Many possible modifications of the inlet geometry have been used in the reduction of swirl. Prior work by Guo and Seddon[2,3] has shown that a large vortex occurs because of flow separation on the bottom wall near the duct throat which produces a large swirl at the engine face. In the prior work, two devices for swirl control were used; one is the solid spoiler, the other is auxiliary inflow by blowing (auxiliary inflow was found to have adverse effects on the flow and pressure recovery characteristics at lower angles of attack). Seddon[4] tested the effect of bottom wall and sidewall fences of various sizes and combinations in reducing the swirl of an S-duct at a 30-deg angle of attack. Tests of Vakili et al.[5] explored the improvement of the secondary flow in an S-duct at 0-deg incidence by using a vortex generator or a flow control rail. The present authors[6] proposed an automatically adjustable blade (AAB) method. The AAB was located inside the duct, and the function relating angle of attack and the optimized angle of the fix (where the duct swirl disappears) was determined. The measures reviewed in the preceding would be invalid or would produce a large total pressure loss when an S-shaped inlet is at a high angle of attack. The flow distortion and duct swirl increase with increasing the angle of attack (up to 80 deg or 115 deg).

This paper describes an improvement of a severely distorted swirl flow in an S-shaped duct at very high angle of attack using a variable lip technique.

Received Jan. 30, 1993; revision received Dec. 15, 1993; accepted for publication Dec. 20, 1993.

*Postdoctoral Fellow, Department of Engineering Mechanics. Senior Member AIAA.

†Professor, Vice President, Department of Aerospace Engineering.

Experimental Description

The S-shaped diffuser investigated is shown in Fig. 1 and consisted of five parts: lip, first bend, straight midsection, second bend, and straight rear section. The diffuser area ratio (exit area to throat area ratio) was 1.3095. Figure 1 also shows the shape and the size of the variable lip device and its location on the model. The lip is 124 mm long, 50 mm wide, and 10 mm thick with a trailing angle of 45 deg. The variable lip is the same shape as those on other walls. It was located at an axial station near the entry where flow separation will occur. The angle of the lip β is 0 deg if the variable lip is close to the wall. The variable lip may change its position by rotation to adjust to the entrance air flow direction. Experimental measurements, including static pressures along the model walls, the cross flow velocities and the total pressure distribution at the diffuser exit were made at α = 0-, 15-, 30-, 45-, 60-, 70-, and 80-deg angles of attack, and compared with test results without the AAB. The tests were performed in a mixed wind tunnel powered by both a vacuum pump and a blower at the Inlet Aerodynamics Laboratory of Nanjing University of Aeronautics and Astronautics. Freestream velocity is about 41.0 m/s. Details of the data processing are described in Ref. 6.

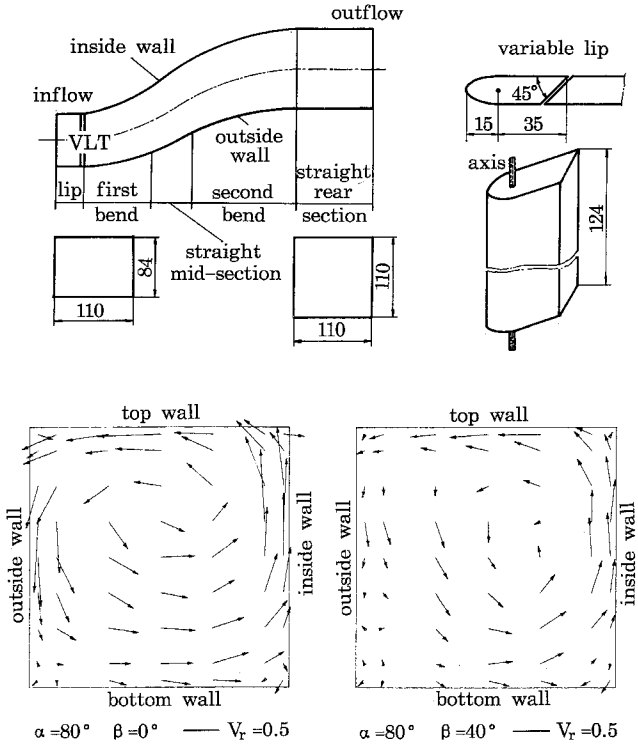

Fig. 1 Experimental model and exit velocity field.

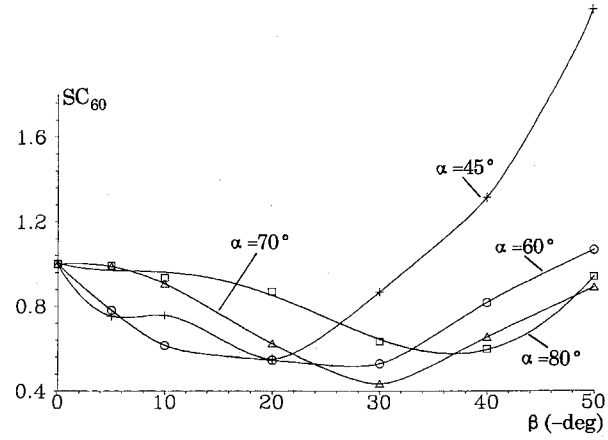

Fig. 2 Variation of SC_{60} with β.